

Developing Nano-Structured Carbon Electrodes for Capacitive Brackish Water Desalination

Linda Zou

*University of South Australia, Adelaide
Australia*

1. Introduction

Capacitive deionisation (CDI) is a promising alternative technology in desalination. It targets to remove the salt ions which are only a small percentage of the feed solution, as compared to most other technologies that aim to shift water which accounts of 90% of the feed solution. As a result, CDI requires less energy to operate and the electrodes are easily regenerated. The basic concept of CDI is electrical potential induced surface adsorption of ions on to electrodes. An electrical field forces charged sodium (Na^+) and chloride (Cl^-) ions in the brackish water to move towards oppositely charged electrodes, by forming electrical double layers, and remove them from the water. It needs low voltage to operate, and it does not require harsh chemical cleaning process. The most critical component of CDI is the carbon electrode materials, as reported that the electrosorptive capacity strongly depends on the physical properties such as surface area and conductivity of the electrode. This chapter reports the current research efforts and progress in the development of porous carbon electrodes conducted in our research group, the commercial activated carbons (ACs), carbon nanotubes (CNTs) including single walled CNTs (SWCNTs) and double walled CNTs (DWCNTs), ordered mesoporous carbons (OMCs), and more recently, graphene nano-flakes were prepared and used as the electrodes of capacitive deionization device. Their salt removal performances were investigated. Their morphology and specific surface area were characterized. The electrosorption experiment results showed that their electrosorptive capacities are in the order of OMCs > SWCNTs > DWCNTs > ACs, ie. 0.93, 0.81, 0.80, 0.62 mg/g respectively. This is attributed to their differences in pore size distribution, pore pattern arrangement and specific surface area. In addition, the ion sorption onto these mentioned materials follows a Langmuir isotherm, indicating monolayer adsorption. Finally, we have investigated the regeneration property of both CNTs and AC through charge-discharge experiment and found that their regeneration was effective.

Chemically modified graphene has been studied in the context of many applications due to its excellent electrical, mechanical and thermal properties. Chemical modification of graphene oxide, which is generated from graphite powder as start material, has been a promising route to achieve mass production of graphene platelets. Hummers and Offeman (1958) developed a powerful oxidation method involving reacting graphite with a mixture of potassium permanganate (KMnO_4) and concentrated sulfuric acid (H_2SO_4) to

achieve an efficient level of oxidation. It is believed that the desalting capacity can be greatly improved by increasing the surface area of the graphene. Recently, graphene-like nano-flakes (GNFs) with relatively high specific surface area have been prepared in our research group and used as electrodes for capacitive deionization. The TEM image of GNFs indicates that GNFs are showing interlayer pattern which is beneficial to ions accessing and adsorbing on the surface of the flakes. Its electrosorptive performance was much better than commercial activated carbon (AC), suggesting a great potential in capacitive deionization application. Further, the electrosorptive performance of GNFs electrodes with different electrical potentials, flow rates and ionic strengths were measured and the electrosorptive isotherm and kinetics were investigated as well. The results showed that GNFs prepared by this process had the specific surface area of 222.01 m²/g. The specific electrosorptive capacity of the GNFs was 1.35mg/g for Na⁺ when the initial concentration was at 25 mg/l, which was higher than that of previously reported data using graphene and AC under the same experimental condition. In addition, the equilibrium electrosorptive capacity was determined as 73.47 μmol/g at 2.0 V by fitting data through the Langmuir isotherm, and the rate constant was found to be 1.01 min⁻¹ by fitting data through pseudo-first-order adsorption. At last, the conductivity of the synthesized graphene materials and activated carbons are determined and then compared by using a four-pin resistivity meter. The results suggested that the chemically synthesized GNFs can be a promising candidate of electrode material in CDI process for brackish water desalination.

2. Current desalination technologies for water challenge

In recent decades, the most widely used processes for desalination have included two membrane separation ones. The list is reverse osmosis (RO), electrodialysis (ED), thermal separations: multistage flash distillation (MSF), multi-effect distillation (MED) and mechanical vapor compression (MVC). Among these processes, RO or MSF methods are employed in the bulk of the seawater desalination plants (90%) worldwide [1]. At membrane based desalination plants, RO occupies 86% while ED only represents 14%. Compared to the thermal systems, membrane processes, such as RO and ED, are widely adopted for desalination from the point view of energy costs [2].

A recent review written by Anderson [2] who has systematically analysed all the information available in the literature regarding energy costs of water desalination. He has pointed out that the ED process is not suitable for water with a concentration of dissolved solids below 400 ppm due to low conductivity. Furthermore, both RO, ED systems require feed pre-treatment to remove species that may, precipitate onto, or otherwise "foul" the surface of the ion exchange membranes and thus decrease the desalination performance of ED as well as RO. Hence, fouling of membranes is still a major challenge for RO and ED technologies.

2.1 Capacitive desalination

Capacitive deionization (CDI) is an electrochemically induced alternative approach for removing salt ions from concentrated aqueous solutions by means of forcing charged ions into the electrical double layer at an electrode-solution interface when the electrode is connected to an external power supply. The schematic mechanism of CDI is shown in Fig.1. The water containing salt ions flows through a pair of charged electrodes and anions and

cations migrate to separately anode and cathode, respectively. As a consequence, the ions are ideally held onto the double layer. No redox process occurs and the process can easily be regenerated when the electrical power is short circuited or even reversed.

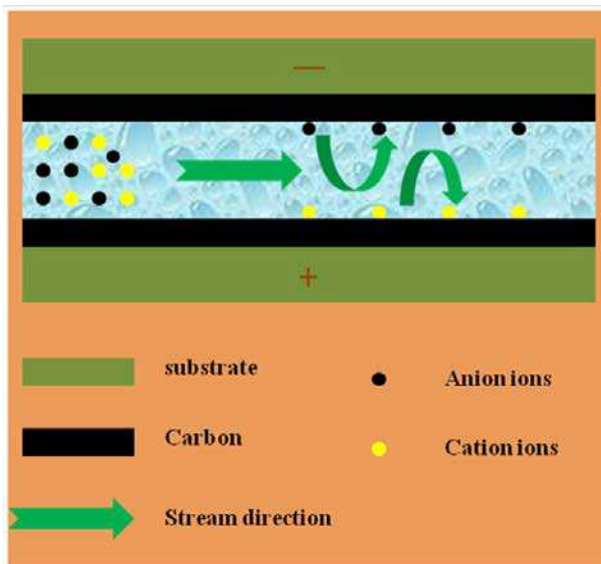


Fig. 1. Schematic diagram of capacitive deionization process

Historically, the double layer was firstly proposed by Helmholtz in 1883 [3], who described the charge distribution between two different phases as a capacitor. Gouy and Chapman then developed the model by considering the gradient of electron density at the charged interface. Later in 1924, the model was completed by Stern by assuming that the double layer can be divided into an “inner” region where the ion distribution followed Langmuir adsorption, while the region further from the surface could be roughly described with the Gouy-Chapman model. Thus, the electrochemical capacitance could be obtained like a series union of inner double layer and diffuse layer contributions.

From the perspective of double layer capacitance, the electrode materials play a crucial role in CDI and therefore to desalination performance. Generally, the electrode is made of porous materials with high specific surface area as well as very good conductivity, both of which will be of great advantage in absorbing large quantities of salt ions for desalination. Regarding the history of CDI, the pioneering work was conducted by the Caudle and Johnson groups in the mid-1960s and the early 1970s [4,5].

More detailed information could be found in a recent review of CDI progress by Oren [6]. Oren has named his version of CDI electrochemical parametric pumping [7,8]. He has published several comprehensive papers analysing the use of new carbon materials in the CDI process as well as fundamental electrochemical double layer issues of the electrodes [9-13]. In the mid-1990s, Farmer and co-workers [14-17] from the Lawrence Livermore National Labs (LLNL), developed a new kind of high specific surface area material which was called carbon aerogel for their CDI device and at the same time rekindled interest in CDI within the scientific community.

In recent years, most reports in terms of CDI typically utilized various carbons, such as carbon aerogels [14-16], carbon cloth [18-20], carbon sheets [21], carbon nanotubes [22-30] and mesoporous carbon [31-34] etc as electrode materials because these materials have the advantage of high specific surface area, easy large scale production and environmental-friendly.

In addition to CDI, membrane capacitive deionization technology (MCDI) as a modification of CDI has attracted great attentions. CDI which combined with an ion exchange membrane has shown great desalination performance compared to CDI without the membrane [35-38]. In a standard CDI device, the salt removal efficiency would be slightly reduced because of co-ion effects (ions of equal polarity as the electrode). These co-ions are near the electrode but cannot be electro-adsorbed efficiently. To avoid this negative effect, ion-exchange membranes have been introduced in front of the electrodes [38]. Specifically, a cation-exchange membrane is placed in front of the electrode that is negatively polarized, and an anion-exchange membrane is placed in front of the positive electrode. Counter-ions can then move freely into and out electrode while co-ion transport is restricted. In this chapter, we will introduce some of typical carbon materials, such as activate carbon, carbon nanotube (single walled and double walled) as well as a new rising star in carbon community "graphene", for application of CDI electrode base on a lab-scale CDI unit. Further, the optimized electrodes' materials were employed to carry out the desalination experiment with MCDI unit. We believe that these would be valuable for industrializing CDI technology in near future.

3. Lab scale CDI Experiments

The typical bench scale CDI unit cell consists of a retaining plate, carbon electrode and spacer which are shown schematically in Fig. 2. To assemble the MCDI unit, the ion-exchange membranes were soaked in distilled water for 2-3 days to make them sufficiently saturate before use and then inserted into either side of the insulated spacer but in front of carbon electrodes. In the adsorption experiments, the solution was pumped into the unit cell by means of peristaltic pump and the effluent returned to the unit cell. The solution volume was maintained at 50 ml and the ambient temperature was kept at 298 K, respectively. Meanwhile, the applied voltage was adjusted from 1.0 V to 2.0 V to determine the optimum working voltage. The above mentioned experiments were performed using a synthetic NaCl solution which had an initial conductivity of around 55 $\mu\text{S}/\text{cm}$. The relationship between conductivity and concentration was established according to a calibration table made prior to the experiment. The concentration variation of NaCl solution was continuously monitored at the outlet of the unit cell by using conductivity meter.

In these experiments, the salt removal capacity and salt removal efficiency were defined as follow, respectively:

$$\text{Salt removal capacity} (\mu\text{mol g}^{-1}) = \frac{(c - c_0)V}{58.44 \times M} \quad (1)$$

$$\text{Salt removal efficiency} (\%) = \frac{(c - c_0)}{c_0} \% \quad (2)$$

Where C and C_0 (mg/l) represent the final and initial concentration, respectively, and V is the volume of the container (ml), and M is the mass of carbon (g).

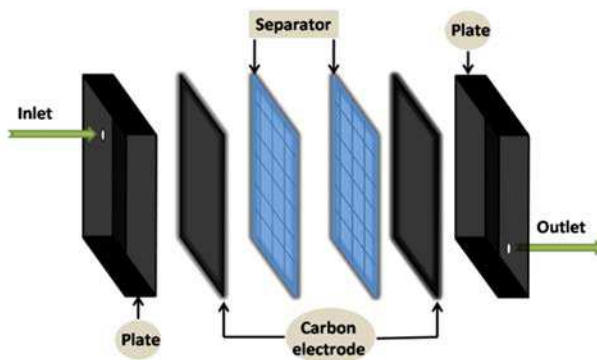


Fig. 2. Schematic diagram of CDI unit

3.1 Fabrication of carbon electrode

In this experiment, commercial ACs and CNTs were employed to fabricate the CDI electrodes. The specifications of as-purchased CNTs are listed in Table 1. The AC/CNTs, graphite as conductive material and PTFE as binder were used to fabricate the CDI electrodes. Their respective percentages in the final electrodes are 72%, 20% and 8%. Each electrode was 70 mm wide \times 140 mm long \times 0.3 mm thick, and had a flow-through hole with a diameter of 4 mm. To achieve adhesion between the carbon mixture and graphite layer, the raw mixture of powders (carbon material, graphite powder and PTFE powder) should be grind for several hours. Ethanol (10-20 ml) was added dropwise to the mixture to make it moist and it was then pressed onto graphite sheet.

Parameters	Double walled carbon nanotube	Single walled carbon nanotube
Diameter	< 5nm	< 2nm
Length	5 ~ 15 μ m	5 ~ 15 μ m
Purity of CNTs	\geq 90%	\geq 90%
Ash	\leq 2wt%	\leq 2wt%
BET	> 400m ² /g	> 400m ² /g
Amorphous Carbon	< 5%	< 5%

Note: the actual specific surface areas of the AC, DWCNTs and SWCNTs characterized by means of a N₂ adsorption system were 999, 415 and 455 m²/g, respectively. The dominant peak present in the pore size distribution was below 1 nm for AC and around 2 nm for CNTs.

Table 1. Specifications of as-purchased CNTs

3.2 Characterization of carbon electrode materials

The structures of the electrode materials were characterized by transmission electron microscopy (TEM, CM200) imaging. The N₂ adsorption-desorption isotherms of the carbon materials were performed at -196°C on a Belsorp system (BEL JAPAN, INC). The pore size distribution curve was calculated by the Barrett-Joyner-Halenda (BJH) method from the desorption branch. The specific surface area was calculated from the adsorption data in the relative pressure interval from 0.04-0.2 using the BET method. The total volume (V) was estimated from the amount adsorbed at a relative pressure of 0.98. Dubinin-Radushkevich

(DR) theory was employed for estimating the micropore volume (V_{mi}), and the as-plot method was used for the external surface area (S_e) and the micropore surface area (S_{mi}). The mesopore fraction was obtained from $(V-V_{mi})$.

3.3 Desalination performance of various carbon electrodes

Fig. 3 presents the conductivity trends at various electrical voltages in AC, DWCNTs and SWCNTs, respectively. As expected, the high voltage resulted in high salt removal efficiency because of high electrostatic force between the relevant ions and the polarized electrode. In all cases, the conductivity reduction becomes much smaller after 30 minutes during adsorption process, implying that the electrodes are close to saturation. It is also observed that the slopes of the adsorption curves in (b) and (c) are higher than that in (a) at corresponding working voltages, indicating that the ions can be transferred easily in CNTs (both in DWCNTs and SWCNTs) due to the superior conductivity of CNTs. This leads to a higher ion adsorption rate. Furthermore, the regeneration curve shows that all electrodes could be regenerated efficiently without electro dialysis occurring at the voltage of 1.2 V. Fig.3 (d) illustrates the salt removal capacity with respect to electrical voltage by using AC, DWCNTs and SWCNTs based CDI. At each given voltage, the salt removal capacity follows the order of SWCNTs > DWCNTs > AC. This can be explained in terms of their respective

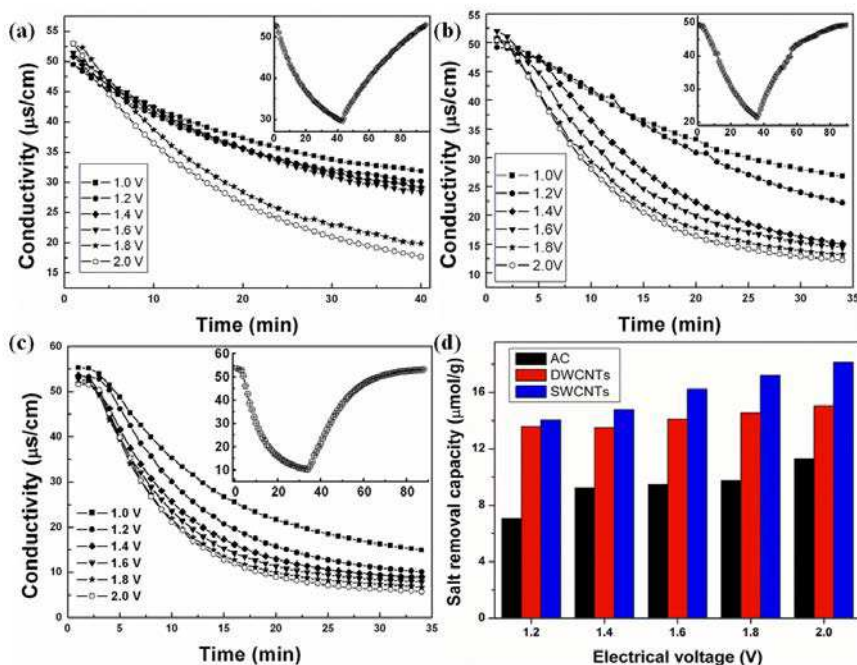


Fig. 3. The conductivity transient in (a) AC (b) DWCNTs and (c) SWCNTs based CDI, respectively. Inset is the corresponding adsorption-desorption curves at an applied voltage of 1.2 V. (d) presents the correlation of salt removal capacity over electrical voltage with an initial conductivity of 80 µS/cm.

pore structures. Although AC has the biggest specific surface area ($999 \text{ m}^2/\text{g}$) among the three targeted materials (compared to $455 \text{ m}^2/\text{g}$ for SWCNTs and $415 \text{ m}^2/\text{g}$ for DWCNTs), but a large fraction of its pores are ascribed to the micropore range according to the IUPAC classification and these are not accessible to ions. It even has a negative effect on salt removal due to the cut-off pore effect. In case of CNTs, the dominant pore sizes are concentrated on 2-3 nm which are ascribed to the mesopore range (2-50 nm) and thereby it is beneficial to electrosorption. In addition, the conductivity at the electrode materials also plays an important role in CDI. Thus, the salt removal strongly depends on many factors, and the most important influence factors are pore size distribution as well as conductivity. Regeneration is another important issue that needs to be considered in evaluating CDI electrode materials. Fig.4 presents the regeneration properties of AC, DWCNTs and SWCNTs. It is noted that all carbon electrodes can be regenerated very well by shorting the circuit. SWCNTs in particular can be regenerated at the level of initial concentration in a very short time. It takes much longer in case of AC electrodes. This can probably be attributed to the weak conductivity and large fraction of micropores. The SWCNTs would be a good candidate electrodes material for CDI. It will also be employed to fabricate MCDI electrode in the following study on MCDI.

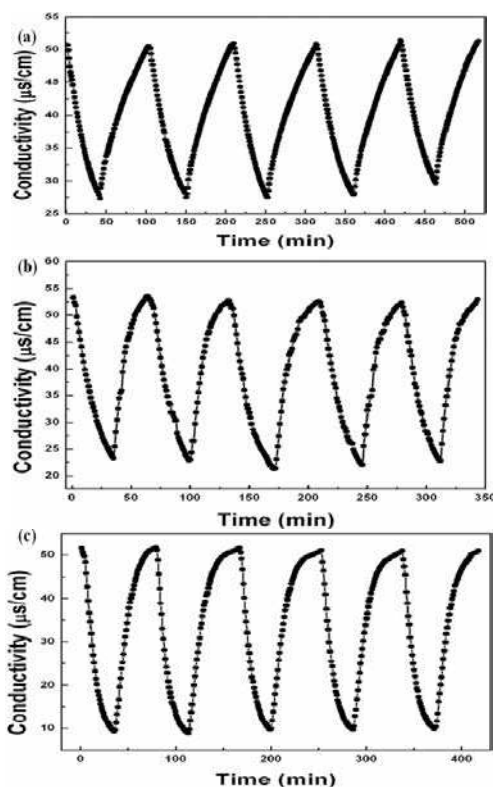


Fig. 4. Regeneration properties of (a) AC, (b) DWCNTs and (c) SWCNTs at an initial salt conductivity of $55 \mu\text{S/cm}$

3.4 Comparison

The TEM images in the Fig. 5 show the ordered porous texture of ordered mesoporous carbon (OMCs, the corresponding CDI data from ref.31), the single and double wall pore structure of CNTs and the random irregular pore arrangement in AC.

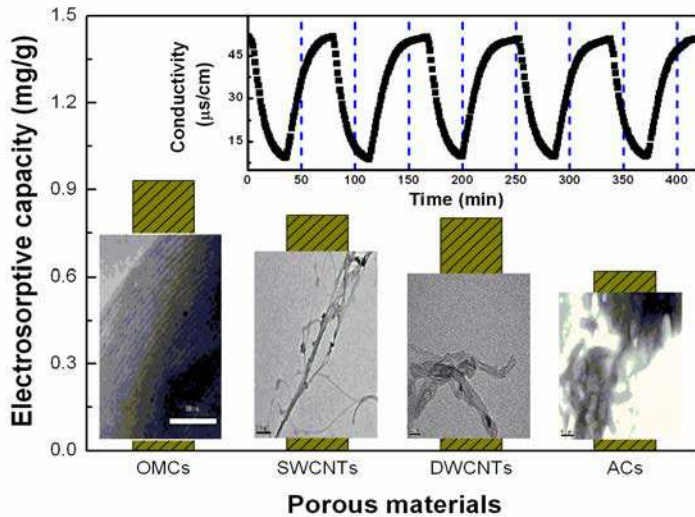


Fig. 5. Comparison of porous carbon materials

Table 2 summarises the characteristics of these four types of porous carbon materials. OMCs have the highest BET surface area of 1491 m²/g, followed by Activated carbon of 845 m²/g, DWCNTs of 413m²/g and SWCNTs of 454m²/g. Although ACs has a higher BET than CNTs, its mean pore size is smaller (2.1nm) than that of both SWCNTs (5.1nm) and DWCNTs (4.8nm). It suggests that ACs have a large amount of micropores whereas OMCs and CNTs both have more mesopores. These differences in pore characteristics have influence on the electrostatic removal of salt ions.

Sample	S _{BET} (m ² /g)	S _{mi} (m ² /g)	V _t (cm ³ /g)	D _{me} (nm)
OMC-S	1491	206	1.589	3.7
AC	845	579	0.605	2.1
DWCNTs	413	307	0.523	5.1
SWCNTs	454	293	0.543	4.8

Table 2. Characteristics of porous carbon materials

During the CDI test, the brackish water flowed through the cell by a peristaltic pump. The experimental results showed that their electrostatic capacities are in the order of OMCs > SWCNTs > DWCNTs > ACs, ie. 0.93, 0.81, 0.80, 0.62 mg/g respectively (Fig. 5). This is attributed to their differences in pore size distribution, pore pattern arrangement and specific surface areas. OMCs and CNTs have pore size that are more suitable for electrostatic adsorption, and more ordered structure that facilitate the easy movement for adsorption

and desorption of Na^+ and Cl^- . In contrast, some surface areas of ACs appear to be unavailable for ion adsorption as the pores are too small to form electrical double layer. In addition, the randomly arranged pore networks of ACs may contribute to the difficulty in the movement of the ions.

3.5 Graphene nanoflakes as electrodes in CDI

3.5.1 Preparation of graphene nanoflakes

Graphite oxide (GO) powders were synthesized by a modified Hummers method [39]. 2.5 g of graphite powder ($<20\mu\text{g}$, Sigma-Aldrich, Inc.) was added into an 353 K solution of a concentrated nitric acid and sulphuric acid mixture with volume ratio of 1:1 (120 ml each), the suspension was mixed for 4.5 h. After that, the mixture was then cooled down to the room temperature and diluted with 0.5 l of deionized (DI) water and left overnight. Later, the mixture was filtered and dried in ambient condition for 24 h. The reaction vessel contained 120 ml of concentrated H_2SO_4 and pre-treated graphite powder was immersed in an ice bath, and potassium permanganate was added slowly. Successively, the mixture was stirred for 2 h, then, after the dilution with DI water, 20 ml 30% H_2O_2 was added to the mixture. The colour of mixture changed into brilliant yellow along with bubbling. Finally, the mixture was filtered and washed with HCl aqueous solution (1:10 in volume) to remove residual metal ions, and washed with DI water until pH equalled 7. Exfoliation was carried out by adding hydrazine and mixing for 24 h at a temperature of 353 K. Successively, the as-prepared graphene suspension was washed several times and filtered carefully, followed by air dry at 333 K, the GNFs obtained were ready to use.

The fabrication of the electrode involved using 72% of the as-synthesized GNFs as electrode material, 20% of graphite as conductive material, and 8% of PTFE powder as binder. Each electrode was pressed into the dimension of 70 mm wide \times 140 mm long \times 0.3 mm thick, and had a flow-through hole with a diameter of 4 mm.

3.5.2 Effect of working conditions on electrosorptive performance of GNFs.

The key factors that affect the electrosorptive performance of Na^+ on the surface of GNFs include the flow rate and bias potential. As expected, higher voltage leads to higher electrosorptive capacity because of stronger Coulombic interaction. Fig.6 (a) shows the electrosorptive performance of GNFs at different bias potentials, and the inset represents the electrosorptive capacity as a function of voltage. With the voltage increased from 0.8 to 2.0 V, the electrosorptive capacity is gradually increased from 4.44 $\mu\text{mol/g}$ to 23.18 $\mu\text{mol/g}$, which is nearly a 5-fold increase. When the applied voltage is at 2.0 V, no visible gas bubbles were observed, indicating that no water electrolysis was taking place. When taking both electrosorptive capacity and energy consumption into account, the optimum working voltage for GNFs based CDI was 2.0 V. Fig.6 (b) depicts the variation of conductivity in solution with flow rate, and the inset demonstrates the correlation between the electrosorptive capacity and flow rate. It is clearly observed from the figures that at a lower flow rate, for example, 15 mL/min, GNFs has a lower electrosorptive capacity of 9.03 $\mu\text{mol/g}$. When the flow rate was increased from 15 mL/min to 25 mL/min, the electrosorptive capacity reached the maximum value of 13.9 $\mu\text{mol/g}$. However, the electrosorptive capacity of GNFs electrode was reduced from 13.9 $\mu\text{mol/g}$ to 8.49 $\mu\text{mol/g}$ when the flow rate was further increased. This was due to the equilibrium between electrostatic force and the driving force in the flow rate of 25 mL/min.

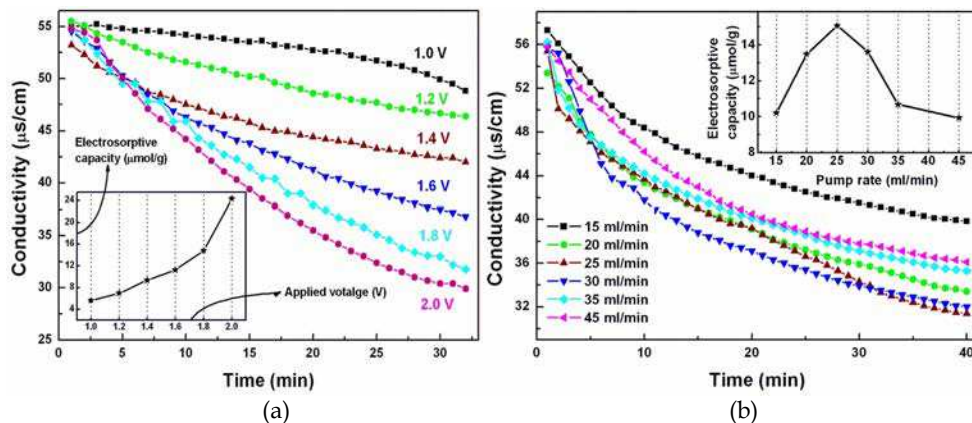


Fig. 6. The electrodesorption of Na⁺ onto GNFs electrode at (a) different bias potentials, (b) different flow rate, respectively, 295 K [40].

3.5.3 Effect of initial concentration on electrodesorptive performance of GNFs

To investigate the electrodesorption behaviour of GNFs, the experiment was carried out at different initial concentrations, and thereby the electrodesorptive isotherm was obtained. The electrodesorption of Na⁺ onto the GNFs electrode was evaluated at a constant temperature of 298 K for the isotherm as well as the kinetic models. The initial concentrations of the NaCl solutions were 25, 50, 100, 250, 400 and 500 mg/l, respectively, as shown in Fig.7. Langmuir Equation (3) and Freundlich Equation (4) were used to validate the experimental data for electrodesorption of Na⁺ onto GNFs, respectively.

$$q = \frac{q_m K_L C}{1 + K_L C} \tag{3}$$

$$q = K_F C^{1/n} \tag{4}$$

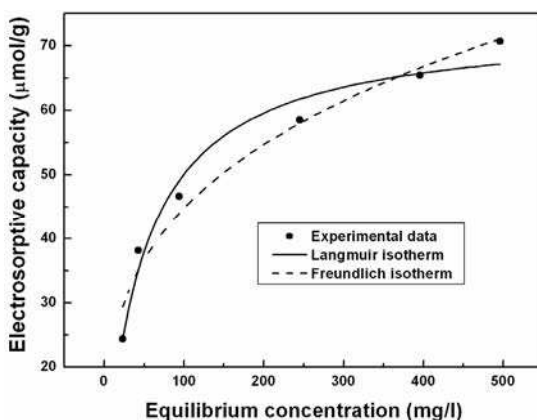


Fig. 7. The electrodesorption isotherm of Na⁺ onto GNFs electrode at 2.0 V [40]

Where C is the equilibrium concentration (mg/L), q is the amount of adsorbed Na^+ (in micromoles per gram of GNFs), q_m is the maximum adsorption capacity corresponding to complete monolayer coverage. It was found that the Langmuir isotherm correlated better with the experimental data according to the r^2 . This phenomenon suggested that the monolayer adsorption was dominant during the electrosorption process. The parameter q_m in the Langmuir isotherm model is considered as the maximum adsorption capacity, as mentioned above. Thus the equilibrium electrosorption capacity, at polarization of 2 V and the flow rate of 25 ml/min, was $73.47 \mu\text{mol/g}$, which is higher than previously reported data.

3.5.4 Comparison of GNFs and AC electrodes

At the applied voltage of 2.0 V, comparative results of the electrosorptive capacity as well as BET surface area between the GNFs and AC based CDI in the same experimental conditions are shown in Fig.8 (a). Although having the larger surface area ($989.54 \text{ m}^2/\text{g}$) than GNFs

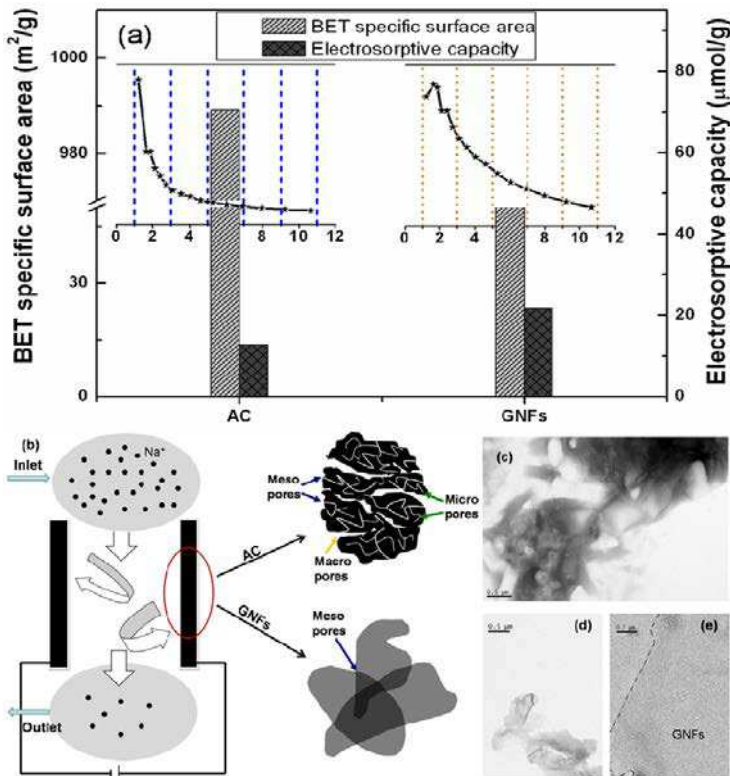


Fig. 8. (a) Comparison of electrosorptive performance by employing GNFs and AC at the same experimental condition, the pictures at top-left and top-right depict the pore size distribution of AC and GNFs below 10 nm, respectively. (b) Mechanism of CDI employing AC and GNFs electrode. TEM observation images of AC (c) and GNFs in low (d) and high (e) magnification, respectively [40].

(222.01 m²/g), AC has an electrosorptive capacity of only 13.73 μmol/g, which is much lower than that of GNFs (whose electrosorptive capacity is 23.18 μmol/g). This can be attributed to the fact that GNFs have an interlayer structure which is more accessible for ions, while AC has a large fraction of inaccessible small micropores. As a result, the effective surface area of GNFs is higher than that of AC. Fig.8 (b) illustrates the principle of CDI and the mechanism of how ions are electrosorbed onto AC and GNFs electrodes, respectively. TEM images of AC and CNFs are used to confirm the hypothesis. The TEM image of GNFs indicates that GNFs are aggregated together, showing a semi-transparent flower shape interlayer pattern. It also shows that GNFs are homogenous flakes with micro-size that are beneficial to ions accessing and are adsorbed on the surface of the flakes. In contrast, the structure of AC on the TEM image shows that it presents a beehive-type pore structure so that the ions cannot access to the inner pores and therefore a high electrosorptive capacity is difficult to achieve. In addition, it is believed that the conductivity of carbon materials also plays a vital role in the electrosorptive process. Having higher bulk conductivity is equivalent to having a higher applied voltage between the two electrodes. It is reported that the conductivity of graphene prepared via chemical approaches is normally above 200 S/m. It is much higher than that of commercial AC whose electrical conductivity is normally between the orders of 10⁻⁶ and 10⁻³ S/m. Further, several experiments regarding conductivity measurement were also performed by measuring GNFs and AC film, respectively and found that the conductivity of GNFs was much better than that of AC. Another possible reason for the high conductivity for GNFs is the presence of conductive graphitized chunks in the GNFs, which was caused by the incomplete grapheme preparation from the graphite precursor. Thus, considering both effective specific surface area and electrical conductivity, it is believed that the GNFs with high specific surface area have the potential as an excellent candidate electrode material for the CDI.

3.6 Removal efficiency of MCDI for the removal of salt from synthetic brackish water

The following experiments were conducted to investigate the salt removal efficiencies of the MCDI device. The initial salt concentration for MCDI testing was 110 μS/cm, as the MCDI is more efficient in reducing the conductivity.

Fig.9 (a) depicts the typical SWCNTs based MCDI process at different working voltages and the corresponding salt removal efficiencies. The salt removal efficiency increased from 91.3 to 98.1% by varying the polarized bias from 0.8 to 1.6 V. However, by taking into account both energy consumption and salt removal efficiency, the optimum working voltage for SWCNTs based MCDI is recommend as 1.2 V. Another useful piece of information relates to MCDI is shown in Fig.9 (a). It is observed that the slopes of the adsorption curve are very steep which indicates a high adsorption rate constant and therefore confirms the theory that the co-ion effects can be significantly reduced by incorporation of ion-exchange membrane. Furthermore, the high adsorption rate constant also indicates that the ions access the electrode faster and thus the desalination process can be completed in a very short time as well as the corresponding regeneration process. In addition, several experiments have also been performed to check the regeneration property of SWCNTs based MCDI. Fig.8 implies that the salt ions in the testing solution can be nearly depleted during the adsorption process and the electrodes are easily regenerated in the desorption process for three adsorption-desorption cycles.

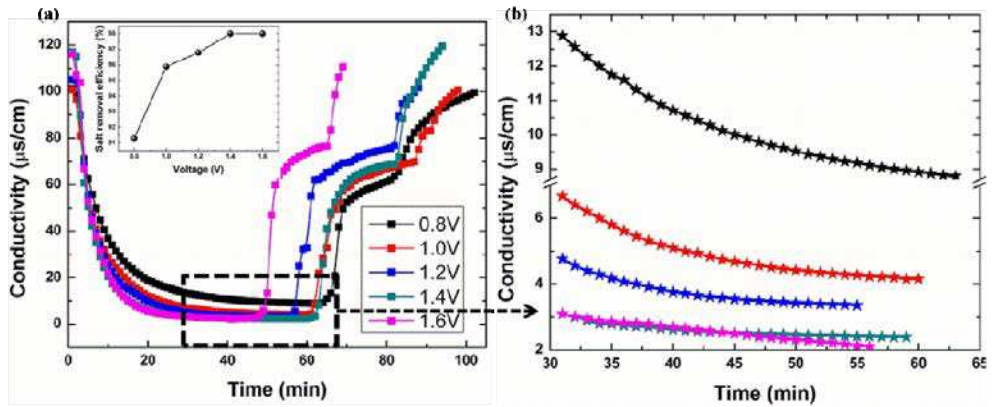


Fig. 9. SWCNTs based MCDI processes at different working voltages (a) (inset shows the corresponding salt removal efficiency) and (b) sorption performance from 30 to 60 minutes. The initial salt concentration was $110 \mu\text{S}/\text{cm}$ [41]

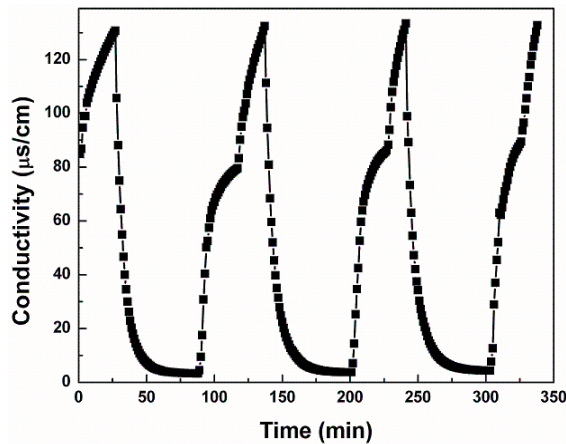


Fig. 10. Regeneration property of SWCNTs based MCDI process at an initial salt concentration of $130 \mu\text{S}/\text{cm}$ [41]

To further investigate the desalination performance of SWCNTs based MCDI at much higher salt concentrations, several experiments were conducted at an initial conductivity of $500 \mu\text{S}/\text{cm}$ and $1000 \mu\text{S}/\text{cm}$ respectively.

Fig.11 (a) shows the conductivity reduction in term of adsorption time at an initial salt conductivity of $500 \mu\text{S}/\text{cm}$. It is noted that the salt removal efficiency increased from 55.4 to 88.2% with the increase of applied voltage from 0.8 to 1.6 V but was still much lower than corresponding salt removal efficiency with lower initial conductivity, for instance, $100 \mu\text{S}/\text{cm}$. Particularly, when the initial conductivity was further increased to $1000 \mu\text{S}/\text{cm}$, the salt removal efficiency continued to decrease as shown in Fig.11 (b). However, the regeneration curve keeps very well by compared with results at low conductivity.

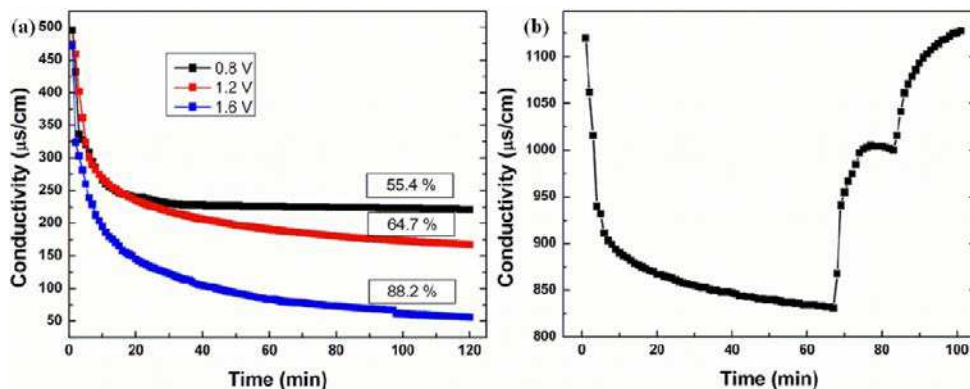


Fig. 11. Desalination performances of SWCNTs based MCDI process at (a) an initial salt conductivity of 500 $\mu\text{S/cm}$ by changing working voltage from 0.8 to 1.6 V (b) an initial conductivity of 1000 $\mu\text{S/cm}$ with applied voltage of 1.2 V [41].

3.7 Comparing desalting results between CDI and MCDI processes

In this section, the SWCNTs based CDI and corresponding MCDI are compared on their desalination performance at the same experimental conditions. The result is showed in Fig.12 which draws the typical adsorption-desorption process based on two devices.

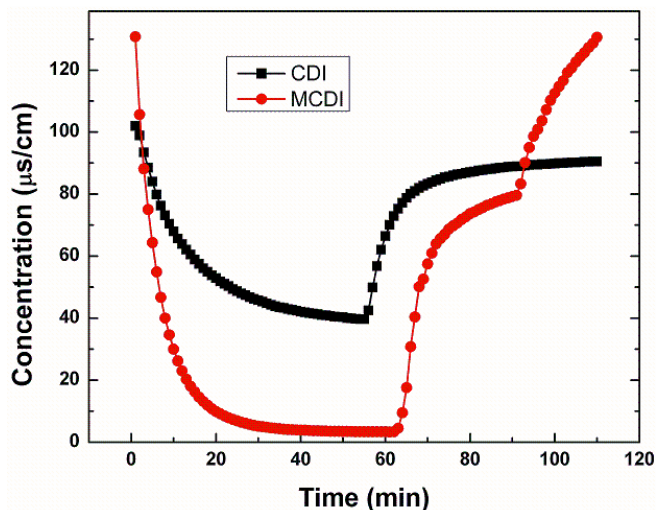


Fig. 12. Comparative desalination result by SWCNTs based CDI and MCDI. (the initial conductivity is around 100 $\mu\text{S/cm}$, the electrical voltage is of 1.2 V, the other experimental conditions are according to the experimetal section) [41]

In Fig.12, the salt conductivity dramatically decreased within first 30 minutes and gradually approached to saturation and then increased to the initial level once the electricity was cut off. Apparently, the salt removal efficiency of CDI (about 60%) is much less than that of

MCDI (about 98%). As discussed in the preceding section, the salt removal efficiency would be affected by co-ions effect. On the other hand, the MCDI is much more beneficial for selective ion transfer as a result of the presence of the ion-exchange membrane and this can be confirmed from the slope of the adsorption curve as well.

4. Conclusions

The electrosorption experiment results of different porous carbon electrodes showed that their electrosorptive capacities are in the order of OMCs >SWCNTs>DWCNTs>ACs, ie. 0.93, 0.81, 0.80, 0.62 mg/g respectively. This is attributed to their differences in pore size distribution, pore pattern arrangement and specific surface areas. It was found that the ion sorption onto these mentioned materials follows a Langmuir isotherm, indicating monolayer adsorption. Finally, the regeneration property of both CNTs and AC were investigated through charge-discharge experiment and it was found that their electrode regenerations were effective. The MCDI is much more beneficial for selective ion transfer as a result of the presence of the ion-exchange membranes and this is confirmed by the more efficient ion adsorption by MCDI than CDI.

Graphene nanoflakes (GNFS) were synthesised by modified Hummer's method. The obtained GNFS were made into electrodes for CDI. Its electrosorptive performance was much better than commercial activated carbon (AC), suggesting to be a good candidate of electrode material in capacitive deionisation application.

5. Acknowledgement

The authors acknowledge the research grants received from Australian Research Council Linkage Grant (LP0883282), Water Quality Research Australia and National Centre of Excellence in Desalination.

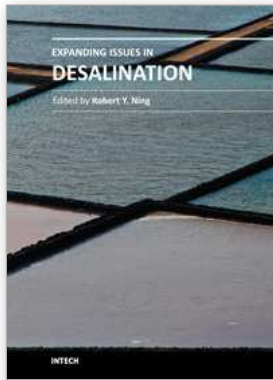
6. References

- [1] Borsani, R.; & Rebagliati, S. (2005). Fundamentals and costing of MSF desalination plants and comparison with other technologies. *Desalination*, Vol.182, No.1-3, pp. 29-37, ISSN 0011-9164
- [2] Anderson, M.A.; Cudero, A.L.; & Palma, J. (2010). Capacitive deionization as an electrochemical means of saving energy and delivering clean water. Comparison to present desalination practices: Will it compete? *Electrochimica Acta* Vol.55, No.12, pp. 3845-3856, ISSN 0013-4686
- [3] Conway, B.E. (1999). *Electrochemical supercapacitors*, Kluwer, ISBN 978-030-6457-36-4, New York, American.
- [4] Caudle, D.D.; Tucker, T.H.; Cooper, J.L.; Arnold, B.B.; & Papastamatakis, A. (1966). Research report Oklahoma university research institute
- [5] Johnson, A.M.; & Newman, J. (1971). Desalting by means of porous carbon electrodes. *Journal of the electrochemical society*, Vol.118, No.3, pp. 510-517, ISSN 0013-4651
- [6] Oren, Y. (2008). Capacitive deionization (CDI) for desalination and water treatment – past, present and future (a review). *Desalination*, Vol. 228, No.1-3, pp. 10-29, ISSN 0011-9164

- [7] Oren, Y. & Soffer, A. (1983). Water desalination by means of electrochemical parametric pumping, separation properties of a multistage column. *Journal of Applied Electrochemistry*, Vol.13, No.4, pp. 489-505, ISSN 0021-891X
- [8] Oren, Y. & Soffer, A. (1978). Electrochemical parametric pumping. *Journal of the Electrochemical Society*, Vol.125, No.6, pp. 869-875, ISSN 0013-4651.
- [9] Oren, Y. & Soffer, A. (1986). The electrical double layer of carbon and graphite electrodes Part III. Charge and dimensional changes at wide potential range. *Journal of Electroanalytical Chemistry*, Vol.206, No.1-2, pp. 101-114, ISSN 1572-6657.
- [10] Cohen, H.; Soffer, A. & Oren, Y. (1987). Adsorption of suspended alumina particles on fibrous carbon and graphite electrodes, *Journal of Colloid and Interface Science*, Vol.120, No.1, pp. 272-280, ISSN 0021-9797
- [11] Oren, Y.; Tobias, H. & Soffer, A. (1983). Removal of bacteria from water by Electroadsorption on porous carbon electrodes. *Bioelectrochemistry and Bionergetics*, Vol.11, No.4-6, pp. 347-354, ISSN 1567-5394
- [12] Oren, Y.; Tobias, H. & Soffer, A. (1984). The electrical double layer of carbon and graphite electrodes, part I: Dependence on electrolyte type and concentration. *Journal of Electroanalytical Chemistry*, Vol.162, No.1-2, pp. 87-99, ISSN 1572-6657
- [13] Oren, Y. & Soffer, A. (1985). The electrical double layer of carbon and graphite electrodes, part II: Fast and slow charging processes, *Journal of Electroanalytical Chemistry*, Vol.186, No.1-2, pp. 63-77, ISSN 1572-6657
- [14] Farmer, J.C.; Fix, D.; Mack, G.; Pekala, R. & Poco, J. (1996). Capacitive deionization of NH_4ClO_4 solutions with carbon aerogel electrodes. *Journal of Applied Electrochemistry*, Vol.26, No.10, pp. 1007-1018, ISSN 0021-891X
- [15] Farmer, J.C.; Fix, D.; Mack, G.; Pekala, R. & Poco, J. (1996). Capacitive Deionization of NaCl and NaNO_3 Solutions with Carbon Aerogel Electrodes. *Journal of the Electrochemical Society*, Vol.143, No.1, pp. 159-169, ISSN 0013-4651
- [16] Farmer, J.C.; Bahowick, S.M.; Harrar, J.E.; Fix, D.V.; Martinelli, R.E.; Vu, A.K. & Carroll, K.L. (1997). Electrosorption of chromium ions on carbon aerogel electrodes as a means of remediating ground water. *Energy and Fuels*, Vol.11, No.2, pp. 337-347, ISSN 0887-0624
- [17] Mayer, S.T.; Pekala, R.W. & Kaschmitter, J.L. (1993). The aerocapacitor: an electrochemical double-Layer energy-storage device. *Journal of the Electrochemical Society*, Vol.140, No.2, pp. 446-451, ISSN 0013-4651
- [18] Ryoo, M.W.; Kim, J.H. & Seo, G. (2003). Role of titania incorporated on activated carbon cloth for capacitive deionization of NaCl solution. *Journal of Colloid and Interface Science*, Vol.264, No.2, pp. 414-419, ISSN 0021-9797
- [19] Oh, H.J.; Lee, J.H.; Ahn, H.J.; Jeong, Y.; Kim, Y.J. & Chi, C.S. (2006). Nanoporous activated carbon cloth for capacitive deionization of aqueous solution. *Thin Solid Films*, Vol.515, No.1, pp. 220 - 225, ISSN 0040-6090
- [20] Ahn, H.J.; Lee, J.H.; Jeong, Y.; Lee, J.H.; Chi, C.S. & Oh, H.J. (2007). Nanostructured carbon cloth electrode for desalination from aqueous solutions. *Materials Science and Engineering A*, Vol.449-451, No.25, pp. 841-845, ISSN 0921-5093
- [21] Park, K.K.; Lee, J.B.; Park, P.Y.; Yoon, S.W.; Moon, J.S.; Eum, H.M. & Lee, C.W. (2007). Development of a carbon sheet electrode for electrosorption desalination. *Desalination*, Vol.206, No.1-3, pp. 86-91, ISSN 0011-9164

- [22] Dai, K.; Shi, L.Y.; Zhang, D.S. & Fang, J.H. (2006). NaCl adsorption in multi-walled carbon nanotube/active carbon combination electrode. *Chemical Engineering Science*, Vol.61, No.2, pp. 428 - 433, ISSN 0009-2509
- [23] Zhang, D.S.; Shi, L.Y.; Fang, J.H.; Dai, K. & Li, X.K. (2006). Preparation and desalination performance of multiwall carbon nanotubes. *Materials Chemistry and Physics*, Vol.97, No.2-3, pp. 415-419, ISSN 0254-0584
- [24] Wang, X.Z.; Li, M.G.; Chen, Y.W.; Cheng, R.M.; Huang, S.M.; Pan, L.K. & Sun, Z. (2006). Electrosorption of ions from aqueous solution with carbon nanotubes and nanofibers composite film electrodes. *Applied Physics Letters*, Vol.89, No.5, PP. 053127-3, ISSN 0003-6951
- [25] Wang, X.Z.; Li, M.G.; Chen, Y.W.; Cheng, R.M.; Huang, S.M.; Pan, L.K. & Sun, Z. (2006). Electrosorption of NaCl solutions with carbon nanotubes and nanofibers composite film electrodes. *Electrochemical Solid-State Letters*, Vol.9 No.9, pp. E23-26, ISSN 1099-0062
- [26] Zhang, D.S.; Shi, L.Y.; Fang, J.H.; Dai, K. & Li, X.K. (2006). Influence of carbonization of hot-pressed carbon nanotube electrodes on removal of NaCl from saltwater solution. *Materials Chemistry and Physics*, Vol.96, No.1, pp. 140-144, ISSN 0254-0584
- [27] Pan, L.K.; Wang, X.Z.; Gao, Y.; Zhang, Y.P.; Chen, Y.W. & Sun, Z. (2009). Electrosorption of anions with carbon nanotube and nanofibre composite film electrodes. *Desalination*, Vol.244, No.1-3, pp. 139-143, ISSN 0011-9164
- [28] Gao, Y.; Li, H.B.; Pan, L.K.; Zhang, Y.P.; Chen, Y.W. & Sun, Z. (2009). Electrosorption behavior of cations with carbon nanotubes and carbon nanofibers composite film electrodes. *Thin Solid Films*, Vol.517, No.5, pp. 1616-1619, ISSN 0040-6090
- [29] Li, H.B.; Pan, L.K.; Zhang, Y.P. & Sun, Z. (2009). Ferric ion adsorption and electrosorption by carbon nanotubes and nanofibers films. *Water Science and Technology*, Vol.59, No.8, pp. 1657-1665, ISSN 0273-1223
- [30] Li, H.B.; Pan, L.K.; Zhang, Y.P.; Zou, L.D.; Sun, C.Q.; Zhan, Y.K. & Sun, Z. (2010). Kinetics and thermodynamics study for electrosorption of NaCl onto carbon nanotubes and carbon nanofibers electrodes. *Chemical Physics Letters*, Vol.485, No.1-3, pp. 161-166, ISSN 0009-2614
- [31] Li, L.X.; Zou, L.D.; Song, H.H. & Morris, G. (2009). Ordered mesoporous carbons synthesized by a modified sol-gel process for electrosorptive removal of sodium chloride. *Carbon*, Vol.47, No.3, pp. 775 -781, ISSN 0008-6223
- [32] Zou, L.D.; Li, L.X.; Song, H.H. & Morris, G. (2008). Using mesoporous carbon electrodes for brackish water desalination. *Water Research*, Vol.42, No.8-9, pp. 2340 - 2348, ISSN 0043-1354
- [33] Lim, J.A.; Park, N.S.; Park, J.S. & Choi, J.H. (2009). Fabrication and characterization of a porous carbon electrode for desalination of brackish water. *Desalination*, Vol.238, No.1-3, pp. 37-42, ISSN 0011-9164
- [34] Richard, T. M.; Costas, T.; James O. Kiggans Jr.; Shannon M.M.; David W.D. & Dai, S. (2010). Hierarchical ordered mesoporous carbon from phloroglucinol-glyoxal and its application in capacitive deionization of brackish water. *Journal of Materials Chemistry*, Vol.20, No.39, pp. 8674-8678, ISSN 0959-9428
- [35] Lee, J.B.; Park, K.K.; Eum, H.M. & Lee, C.W. (2006). Desalination of a thermal power plant wastewater by membrane capacitive deionization. *Desalination*, Vol.196, No.1-3, pp. 125-134, ISSN 0011-9164

- [36] Li, H.B.; Gao, Y.; Pan, L.K.; Zhang, Y.P.; Chen, Y.W. & Sun, Z. (2008). Electrosorptive desalination by carbon nanotubes and nanofibres electrodes and ion-exchange membranes. *Water Research*, Vol.42, No.20, pp. 4923 - 4928, ISSN 0043-1354
- [37] Kim, Y.J. & Choi, J.H. (2010). Improvement of desalination efficiency in capacitive deionization using a carbon electrode coated with an ion-exchange polymer. *Water Research*, Vol.44, No.3, pp. 990 - 996, ISSN 0043-1354
- [38] Biesheuvel, P.M. & Van der Wal, A. (2010). Membrane capacitive deionization. *Journal of Membrane Science*, Vol.346, No.2, pp. 256-262, ISSN 0376-7388
- [39] William, S.; Hummers, J. & Offeman, R.E. (1958). Preparation of graphitic oxide. *Journal of the American Chemical Society*, Vol.80, No.6, pp. 1339-1341, ISSN 0002-7863
- [40] Li, H.B.; Zou, L.D.; Pan, L.K. & Sun, Z. (2010). Novel Graphene-Like Electrodes for Capacitive Deionization. *Environmental Science and Technology*, Vol.44, No.22, pp. 8692-8697, ISSN 0013-936X
- [41] Li, H.B. & Zou, L.D. (2011). Ion-exchange Membrane Capacitive Deionization: A New Strategy for Brackish Water Desalination, *Desalination*, Accepted, ISSN 0011-9164



Expanding Issues in Desalination

Edited by Prof. Robert Y. Ning

ISBN 978-953-307-624-9

Hard cover, 412 pages

Publisher InTech

Published online 22, September, 2011

Published in print edition September, 2011

For this book, the term “desalination” is used in the broadest sense of the removal of dissolved, suspended, visible and invisible impurities in seawater, brackish water and wastewater, to make them drinkable, or pure enough for industrial applications like in the processes for the production of steam, power, pharmaceuticals and microelectronics, or simply for discharge back into the environment. This book is a companion volume to “Desalination, Trends and Technologies”, INTECH, 2011, expanding on the extension of seawater desalination to brackish and wastewater desalination applications, and associated technical issues. For students and workers in the field of desalination, this book provides a summary of key concepts and keywords with which detailed information may be gathered through internet search engines. Papers and reviews collected in this volume covers the spectrum of topics on the desalination of water, too broad to delve into in depth. The literature citations in these papers serve to fill in gaps in the coverage of this book. Contributions to the knowledge-base of desalination is expected to continue to grow exponentially in the coming years.

How to reference

In order to correctly reference this scholarly work, feel free to copy and paste the following:

Linda Zou (2011). Developing Nano-Structured Carbon Electrodes for Capacitive Brackish Water Desalination, Expanding Issues in Desalination, Prof. Robert Y. Ning (Ed.), ISBN: 978-953-307-624-9, InTech, Available from: <http://www.intechopen.com/books/expanding-issues-in-desalination/developing-nano-structured-carbon-electrodes-for-capacitive-brackish-water-desalination>

INTECH
open science | open minds

InTech Europe

University Campus STeP Ri
Slavka Krautzeka 83/A
51000 Rijeka, Croatia
Phone: +385 (51) 770 447
Fax: +385 (51) 686 166
www.intechopen.com

InTech China

Unit 405, Office Block, Hotel Equatorial Shanghai
No.65, Yan An Road (West), Shanghai, 200040, China
中国上海市延安西路65号上海国际贵都大饭店办公楼405单元
Phone: +86-21-62489820
Fax: +86-21-62489821

© 2011 The Author(s). Licensee IntechOpen. This chapter is distributed under the terms of the [Creative Commons Attribution-NonCommercial-ShareAlike-3.0 License](#), which permits use, distribution and reproduction for non-commercial purposes, provided the original is properly cited and derivative works building on this content are distributed under the same license.